Supplement of Atmos. Chem. Phys., 21, 3395–3425, 2021
https://doi.org/10.5194/acp-21-3395-2021-supplement

Supplement of

Future changes in isoprene-epoxydiol-derived secondary organic aerosol (IEPOX SOA) under the Shared Socioeconomic Pathways: the importance of physicochemical dependency

Duseong S. Jo et al.

Correspondence to: Duseong S. Jo (duseong.jo@colorado.edu)

1 Isoprene emission comparison

We compared the annual isoprene emissions for 2011–2013 simulated by CESM2.1.0/MEGANv2.1 and by OMI top-down estimate (Bauwens et al. 2016, available at: http://emissions.aeronomie.be/index.php/omi-based, last access: 1 March 2021). As shown in Figure S2c, CESM2.1.0/MEGANv2.1 overestimates isoprene emissions over the Tropics and underestimates them at high latitudes in the Northern Hemisphere. In terms of magnitude, isoprene emissions over the Tropics are important. We scaled down Tropical isoprene emissions by reducing emission factors of Tropical plant functional types (PFT). Two PFTs were used in the Community Land Model version 5 (CLM5): "broadleaf evergreen tropical tree" and "broadleaf deciduous tropical tree". These two PFTs contribute ~80% of total global isoprene emissions (Guenther et al. 2012). There were still regional discrepancies between CESM2.1.0/MEGANv2.1 and top-down estimates (Figures S2d and S2e), but the global total emission amount became closer to the total emission value by the OMI top-down estimate. Global total annual isoprene emissions changed from 439 Tg yr^{-1} to 260 Tg yr^{-1}, which was comparable to the top-down estimate (266 Tg yr^{-1}).

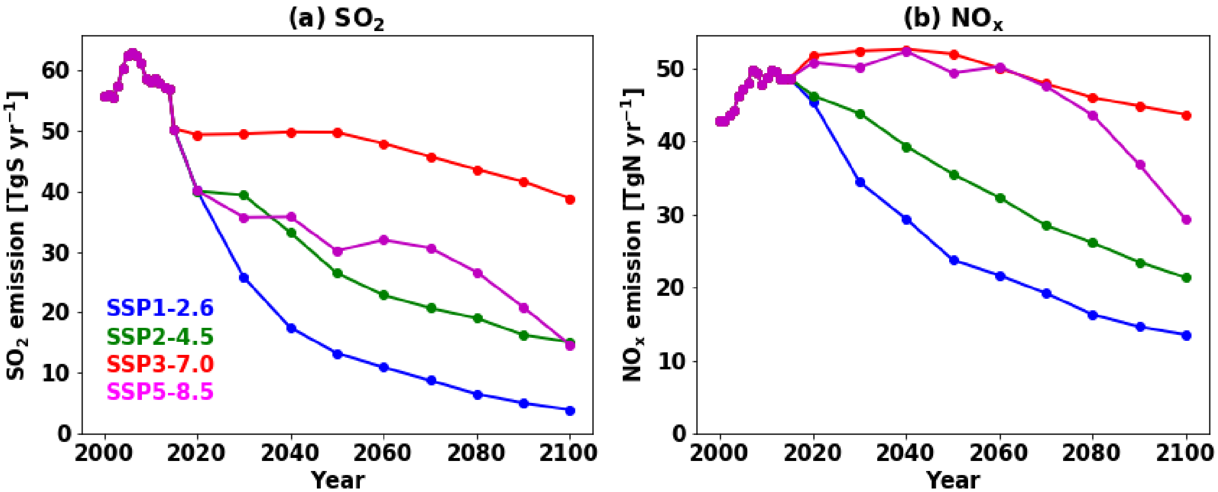

Figure S1. Emission trajectories for SO_2 and NO_x for the four Tier 1 scenarios used in this study.

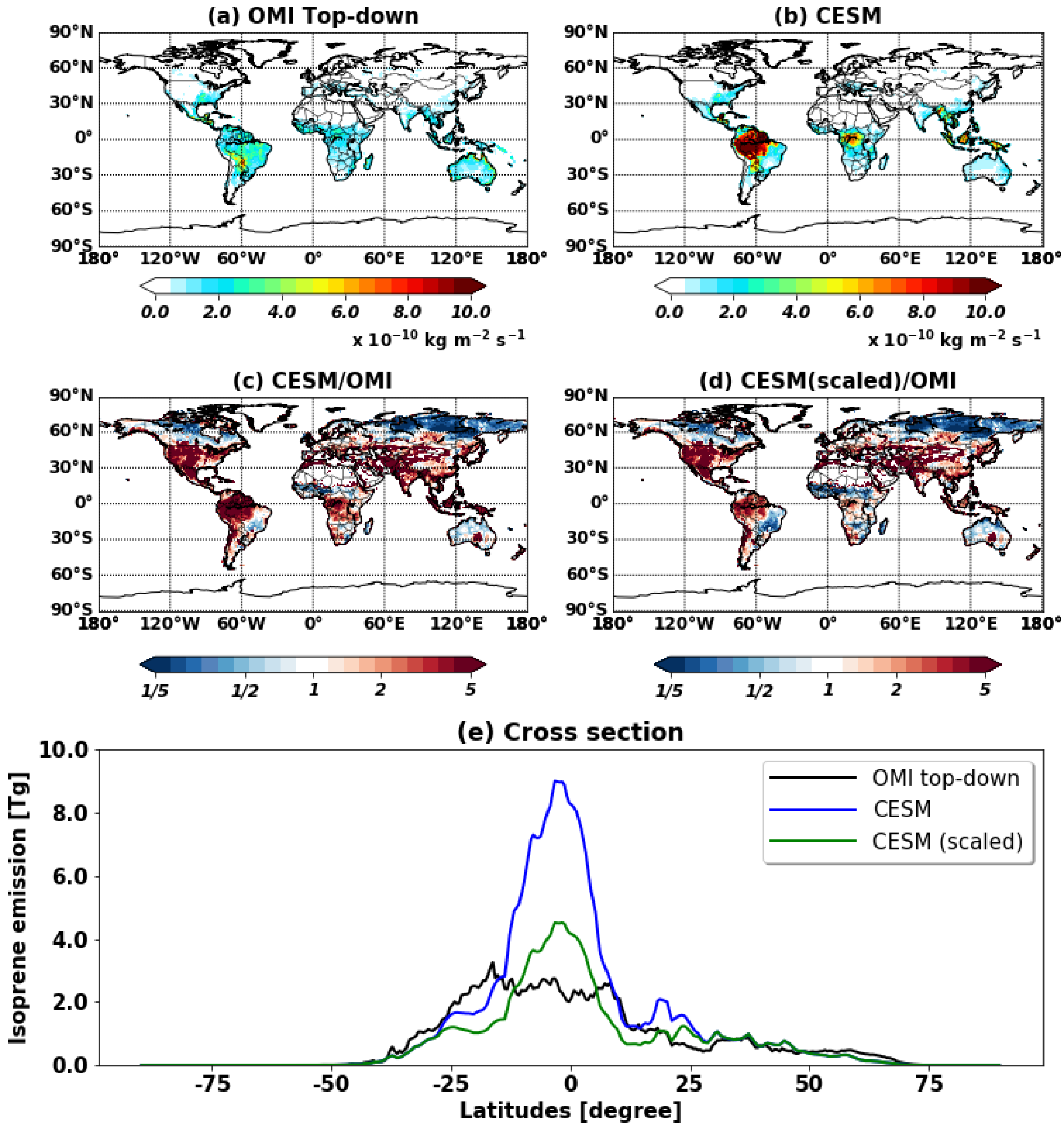

Figure S2. Annual isoprene emissions for 2011–2013 by (a) OMI top-down and (b) CESM2.1.0/MEGANv2.1. (c) Ratios of CESM2.1.0/MEGANv2.1 to OMI top-down isoprene emissions. (d) same as (c) but the isoprene emission factors of tropical trees in CESM2.1.0/MEGANv2.1 are reduced by 50%. (e) Zonal mean cross-section of annual isoprene emissions.

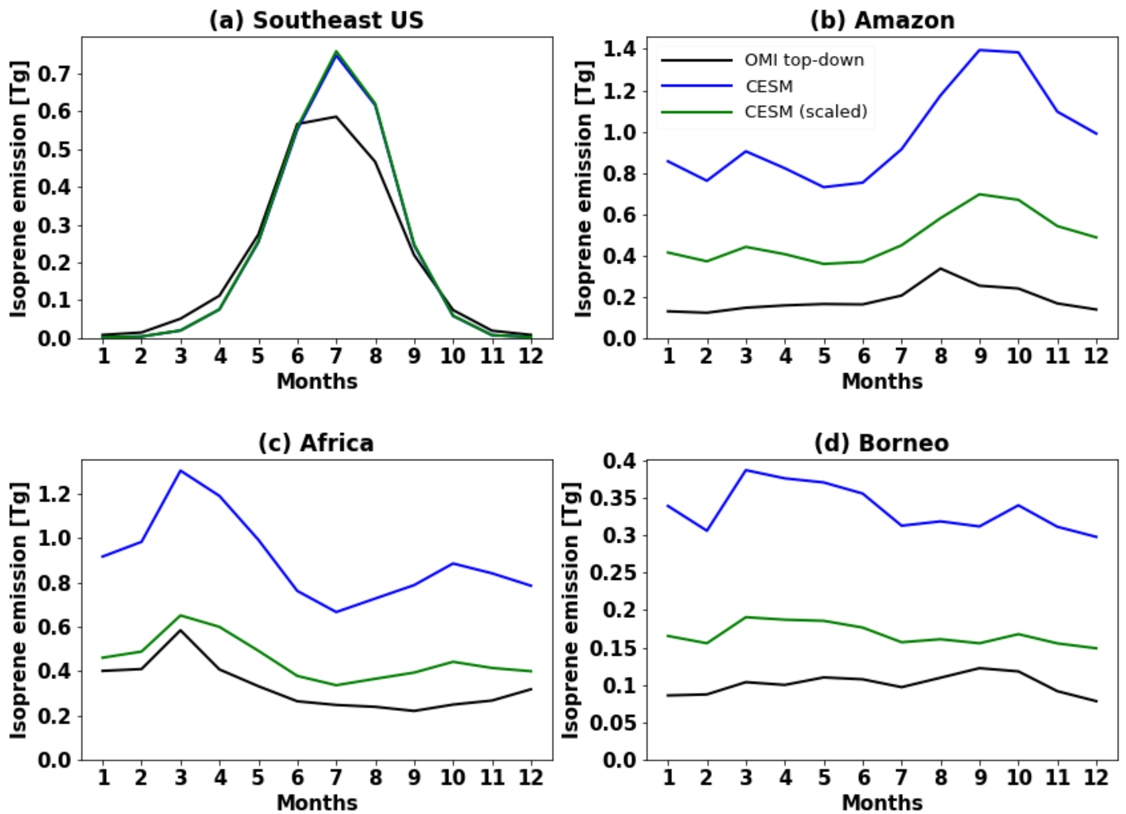

Figure S3. Time series of Isoprene emissions (2011–2013) over (a) Southeast US (30–40°N, 100–80°W), (b) Amazon (10–0°S, 70–60°W), (c) Africa (5°S–5°N, 10–30°E), and (d) Borneo (5°S–5°N, 105–120°E).

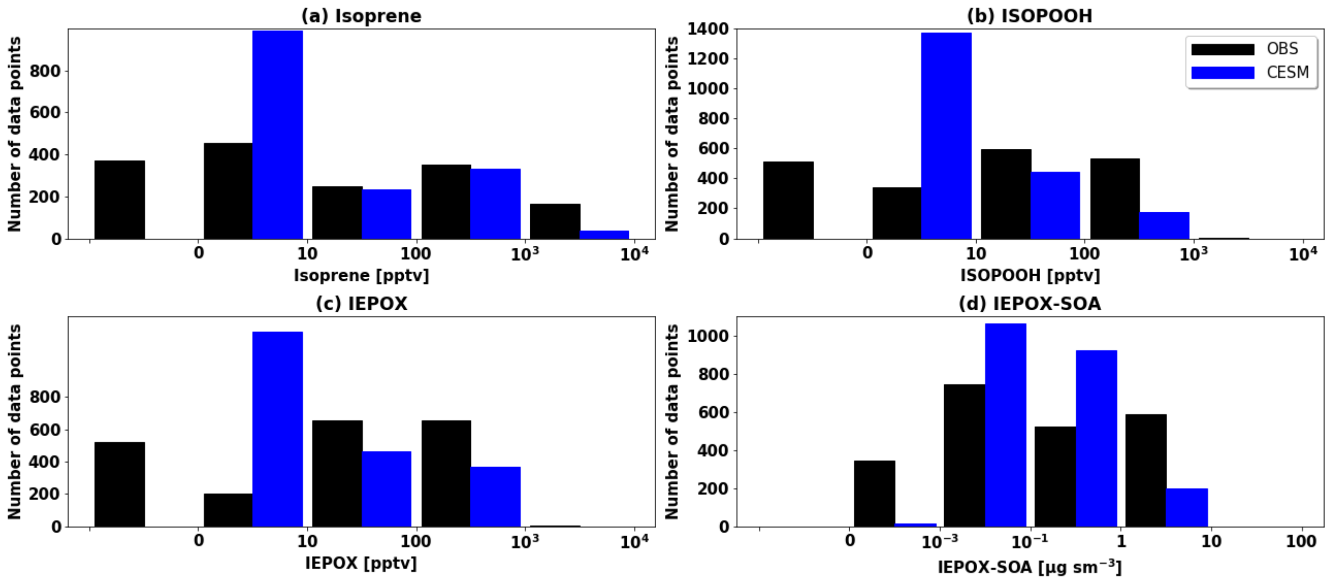

Figure S4. Histograms for observed and modeled (a) isoprene, (b) ISOPOOH, (c) IEPOX, and (d) IEPOX-SOA concentrations during the SEAC4RS campaign. Observation and model results are shown in black and blue bars, respectively. We note that gas measurements can be negative when the real concentrations are zero or very low due to instrumental noise. On the other hand, IEPOX-SOA concentrations were calculated by the positive matrix factorization method and always positive.

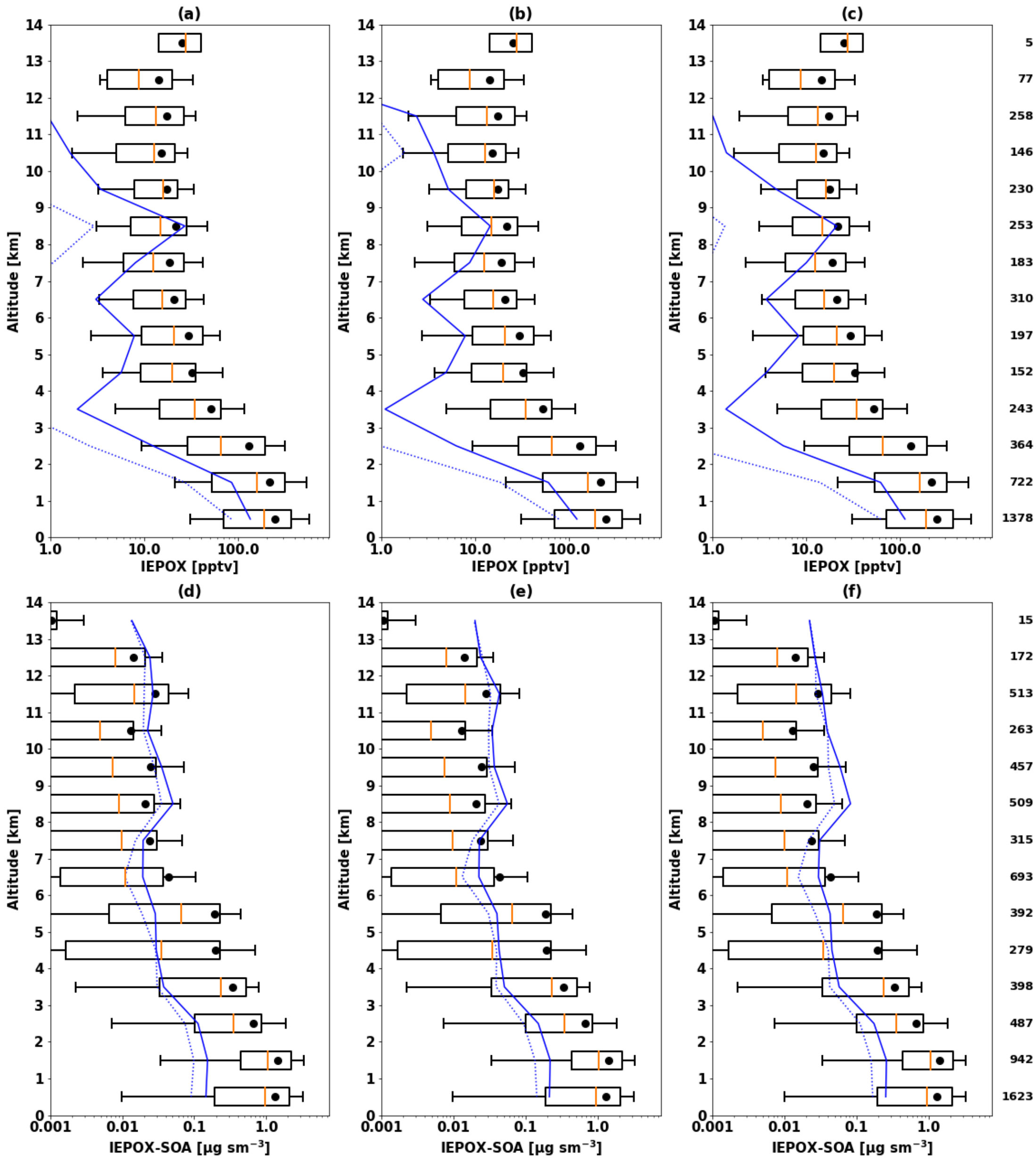

Figure S5. Same as Fig. 1 (c,d) but used different H* values. 8.5×10^7 , 8.5×10^8, 8.5×10^9 M atm^{-1}, are used for (a,d), (b,e), and (c,f), respectively. SOA yield from IEPOX reactive uptake was assumed to be 0.2. IEPOX comparisons are shown in top panels (a,b,c) and IEPOX-SOA in bottom panels (d,e,f).

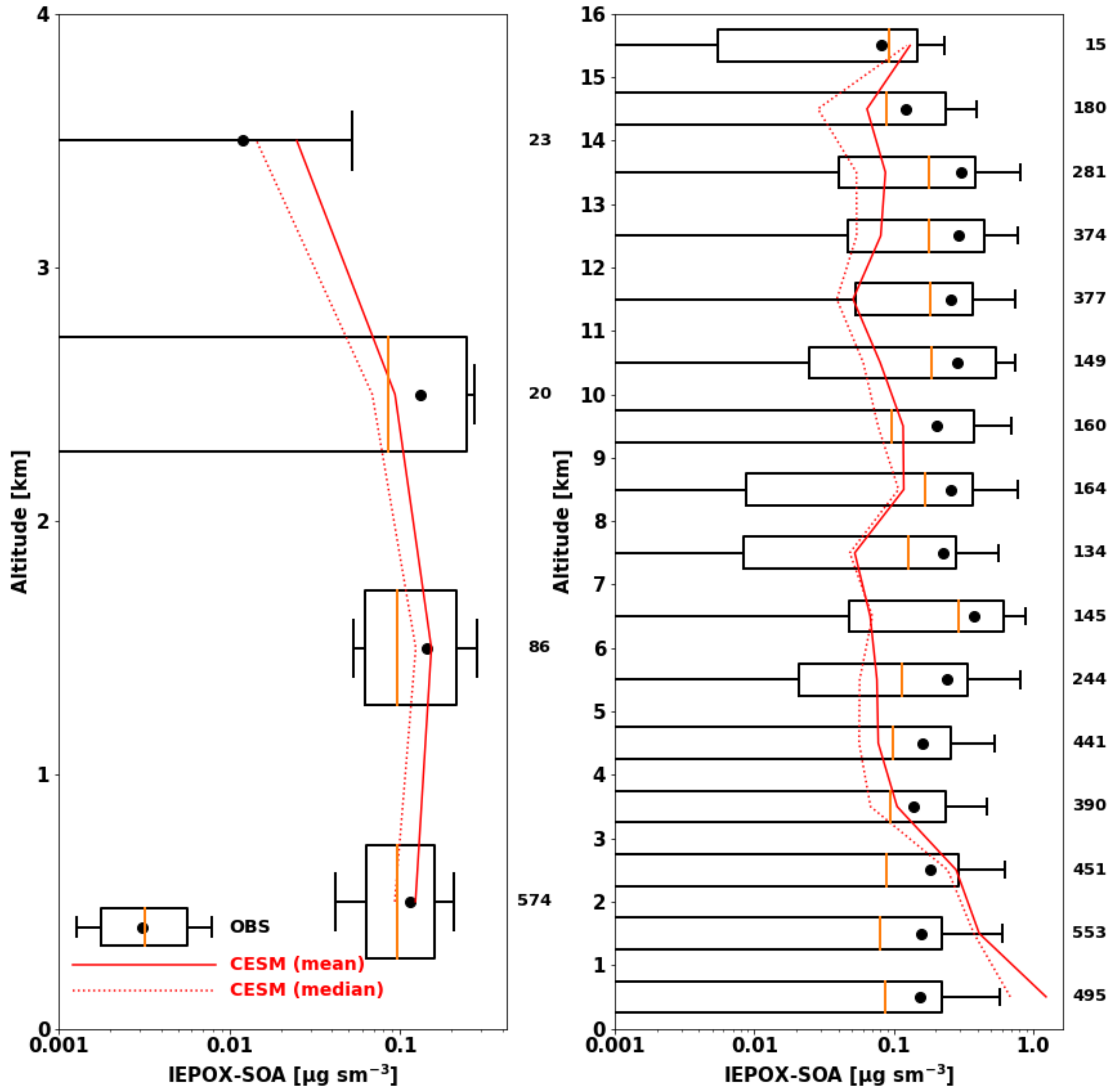

Figure S6. Same as Fig. 2 (c) and (d) but used H^* of 8.5×10^7 M atm^{-1} and the yield of 0.2. The model with the half isoprene emission case (red) is only shown.

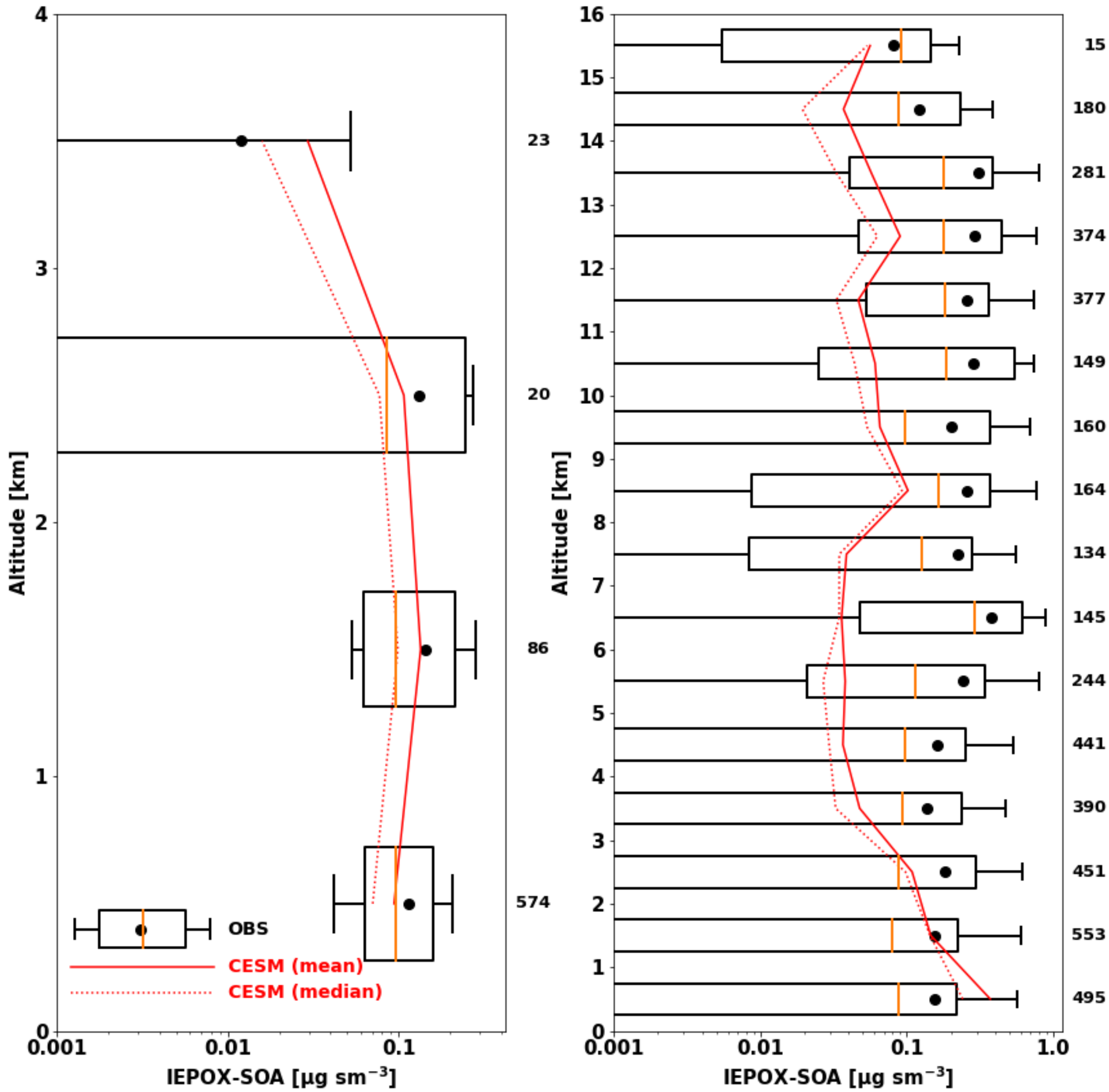

Figure S7. Same as Fig. S6 but assumed 90% of inorganic sulfates are converted to organic sulfates.

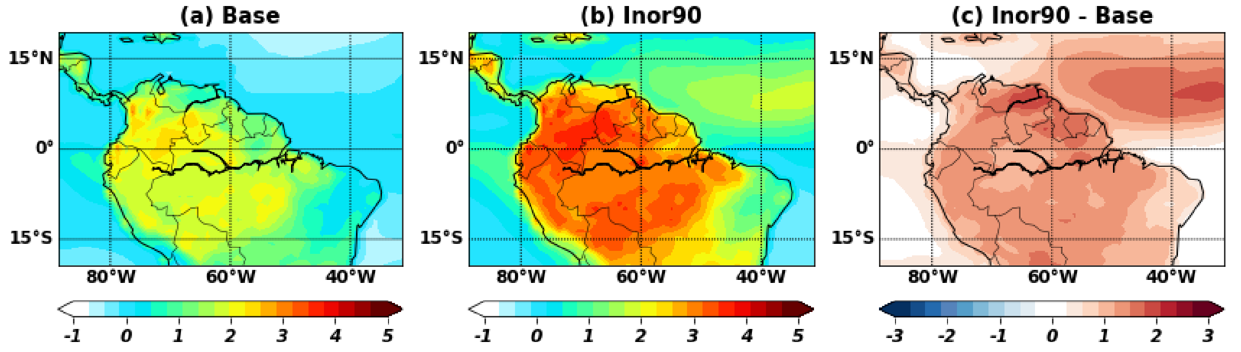

Figure S8. Annual mean aerosol pH at the surface for the year 2010 as simulated by CESM2 model. (a) Base case used in the paper (Base), (b) assuming 90% of inorganic sulfates are converted to organosulfates (Inor90), (c) difference between (a) and (b).

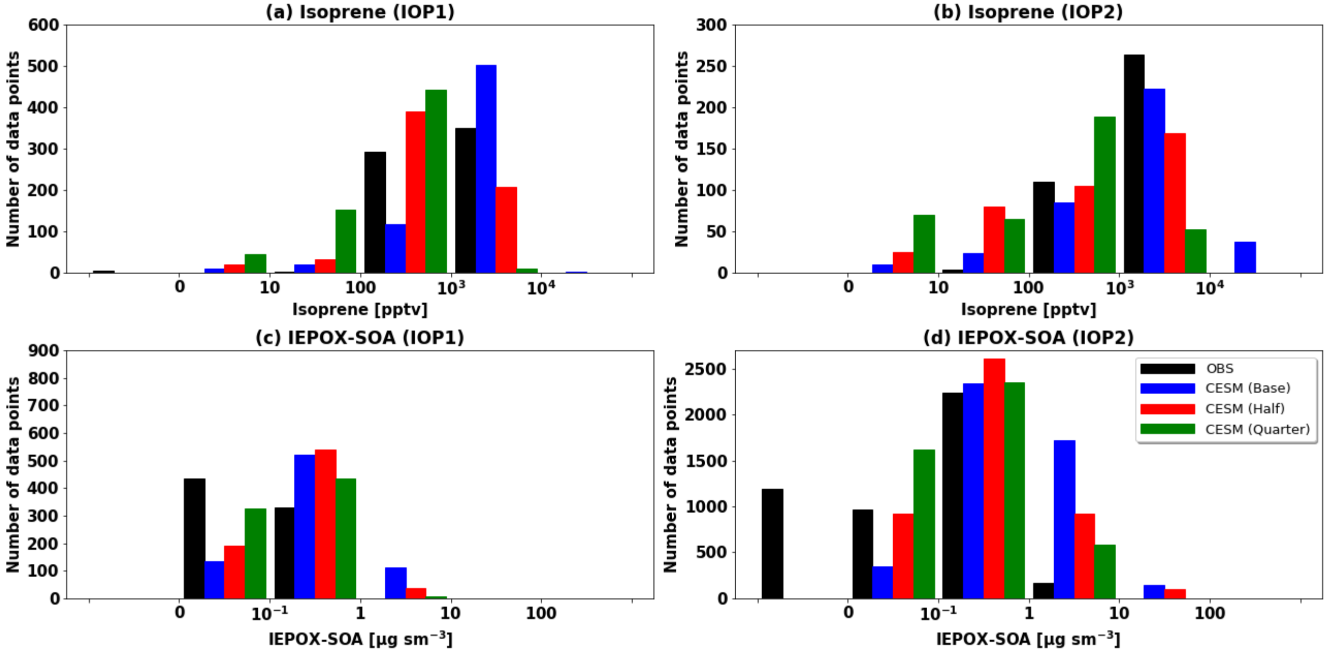

Figure S9. Histograms for observed and modeled (a,b) isoprene and (c,d) IEPOX-SOA concentrations during the GoAmazon campaign. Observations are shown in black bars, and CESM results with different isoprene emissions sensitivities are represented in blue (Base), red (Half), and green (Quarter) bars.

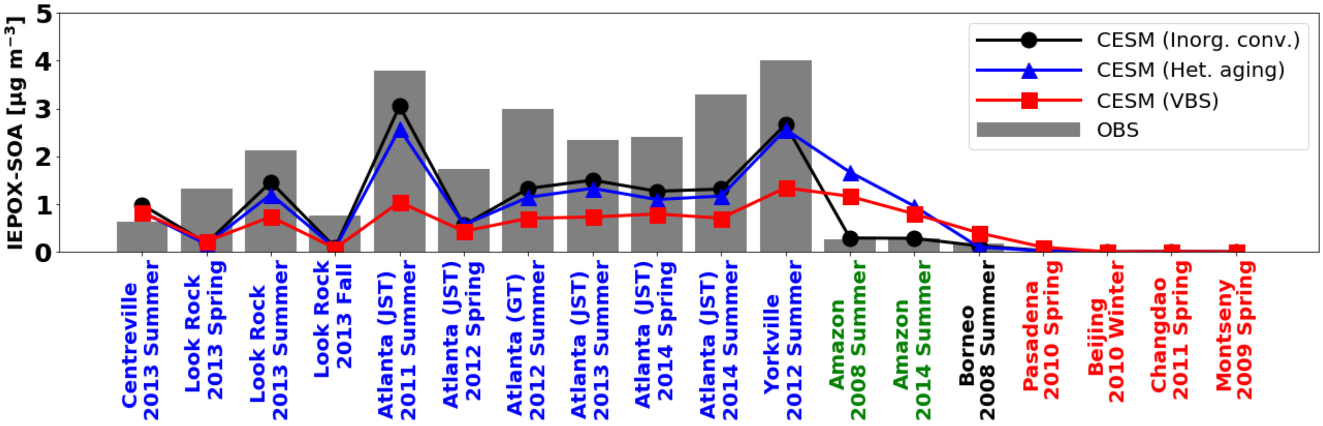

Figure S10. Same as Fig. 3 but for (a) the sensitivity model run with 90% of inorganic sulfate conversion to organic sulfate over the Amazon (black line), (b) the sensitivity model run with heterogeneous OH oxidation of IEPOX-SOA using the rate constant of 4.0×10^{-13} cm^3 $molec.^{-1}$ s^{-1} (blue line), and (c) IEPOX-SOA simulated by the VBS scheme (red line). For the VBS results, SOA from the isoprene + OH pathway was assumed as IEPOX-SOA. We assumed all aged IEPOX-SOA was lost via the fragmentation process for the heterogeneous OH reaction sensitivity run.

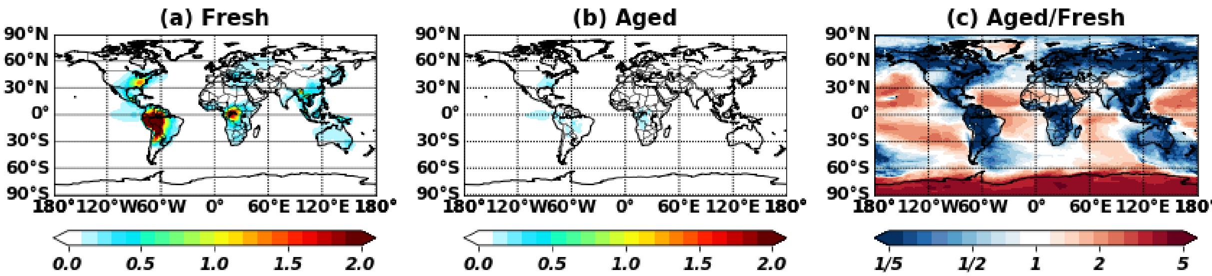

Figure S11. Simulated annual mean IEPOX-SOA concentrations at the surface. (a) Fresh IEPOX-SOA (b) Aged IEPOX-SOA (after heterogeneous oxidation against OH). The ratios between fresh and aged IEPOX-SOA are presented in panel (c). Aged IEPOX-SOA was assumed to be not evaporated and only lost via wet and dry depositions in the model.

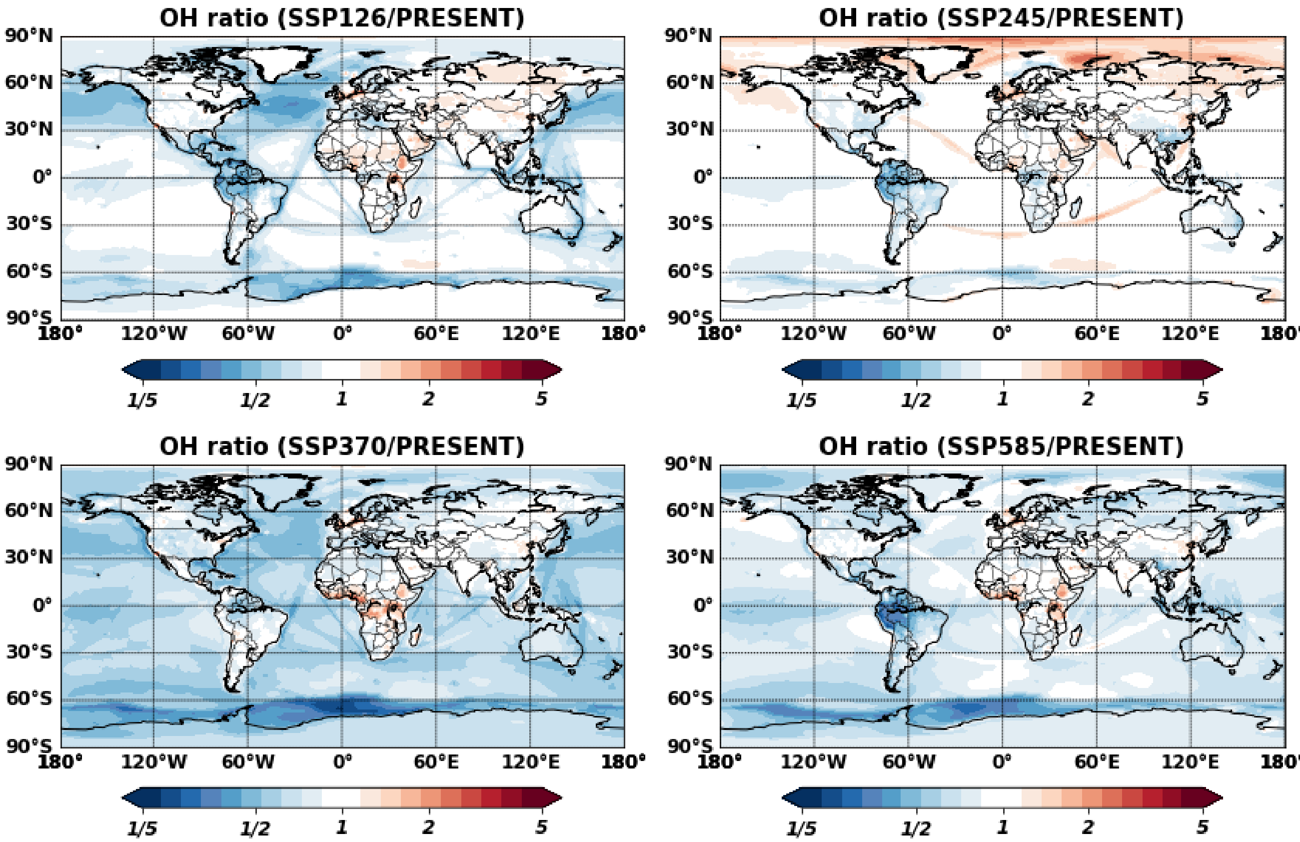

Figure S12. Global ratios of OH simulated under future SSP scenarios (2090s) to present conditions (2010s) at the surface (Explicit case).

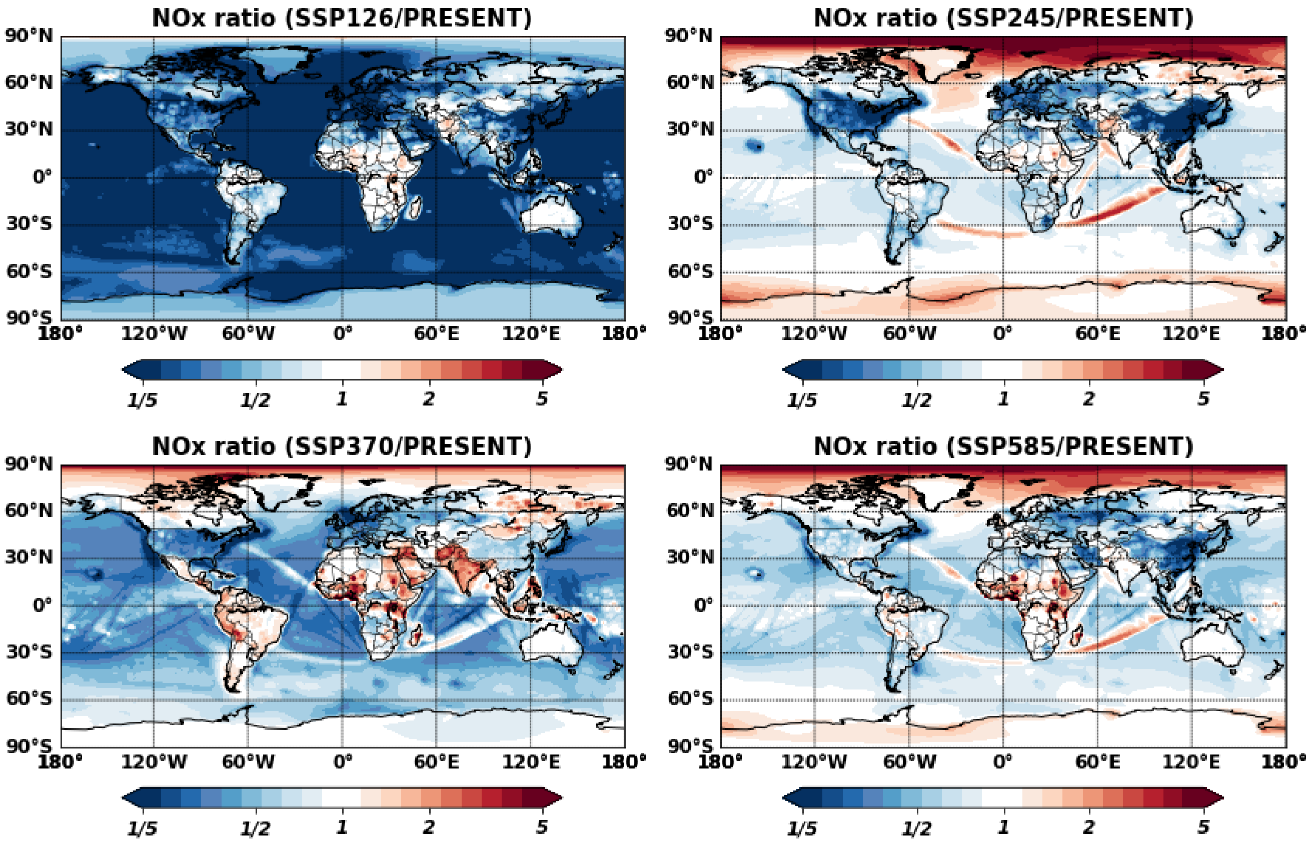

Figure S13. Global ratios of NO_x under future SSP scenarios (2090s) to present conditions (2010s) at the surface (Explicit case).

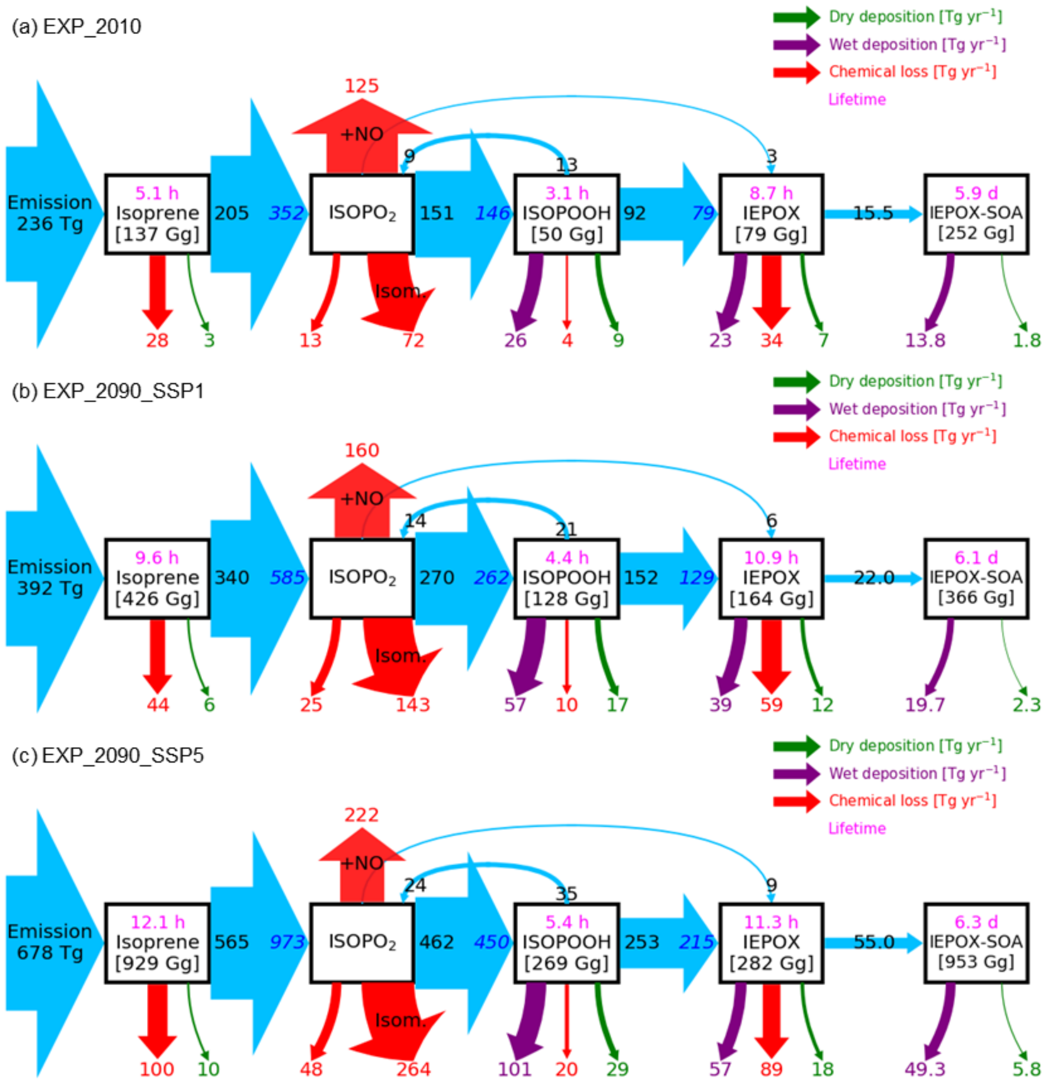

Figure S14. Same as Fig. 6 but for absolute values of mass fluxes (in Tg yr^{-1}).

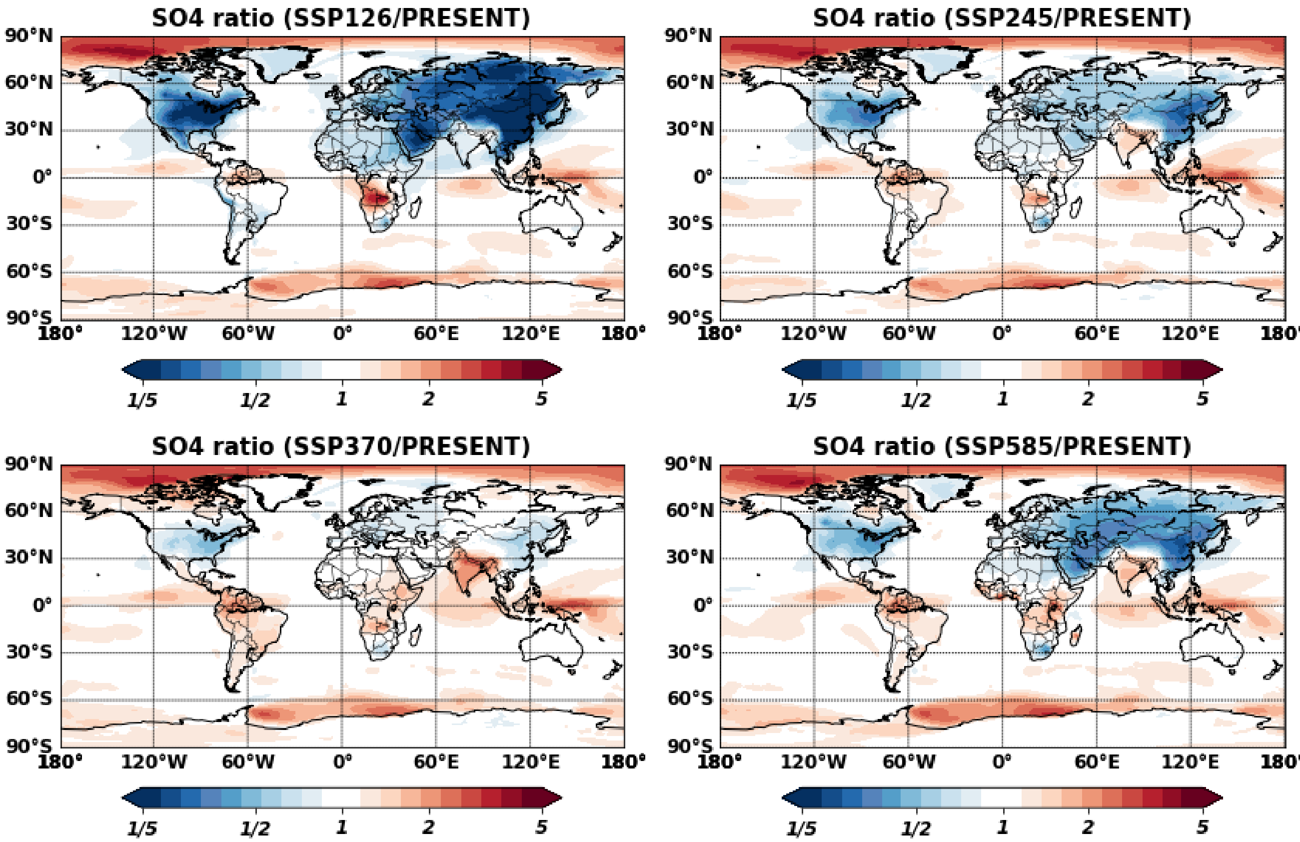

Figure S15. Global ratios of sulfate aerosols under future SSP scenarios (2090s) to present conditions (2010s) at the surface (Explicit case).

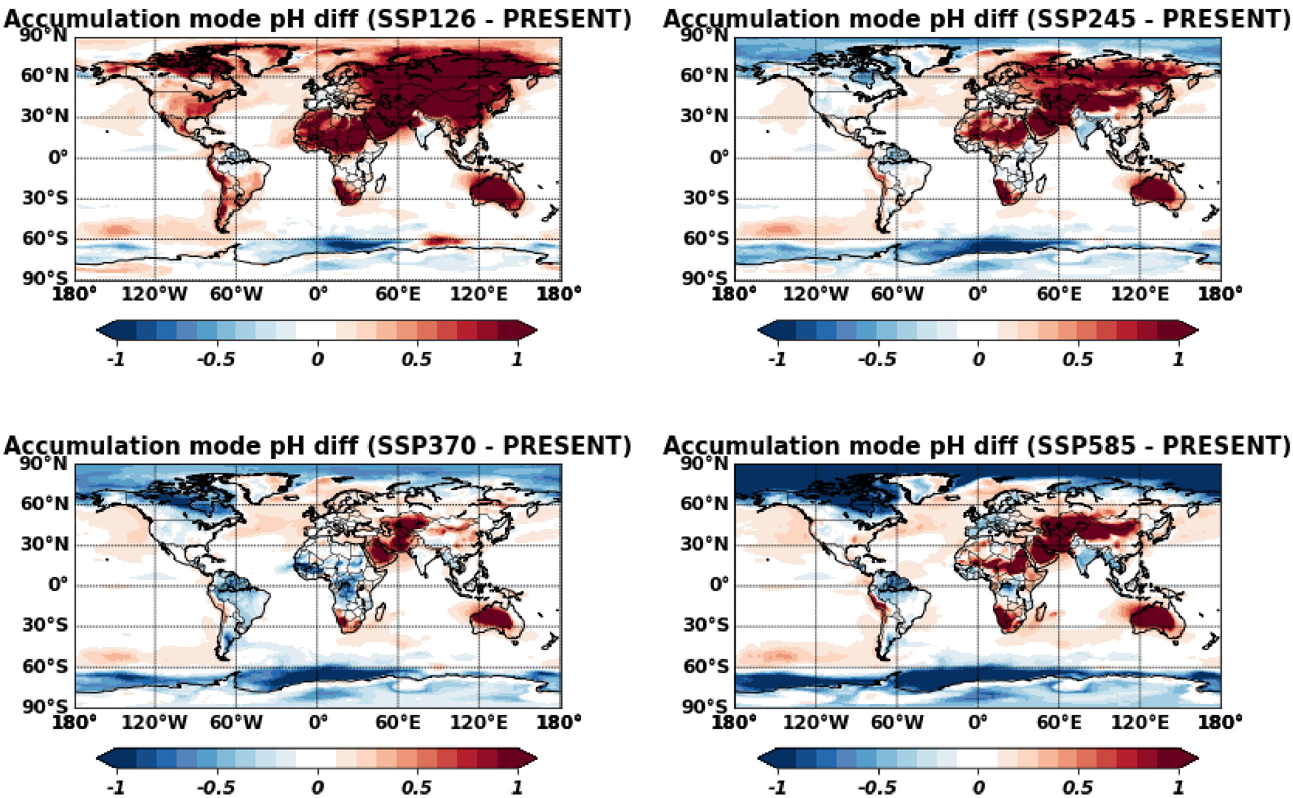

Figure S16. The global aerosol pH (accumulation mode) differences between future SSP scenarios (2090s) and present conditions (2010s) at the surface (Explicit case).

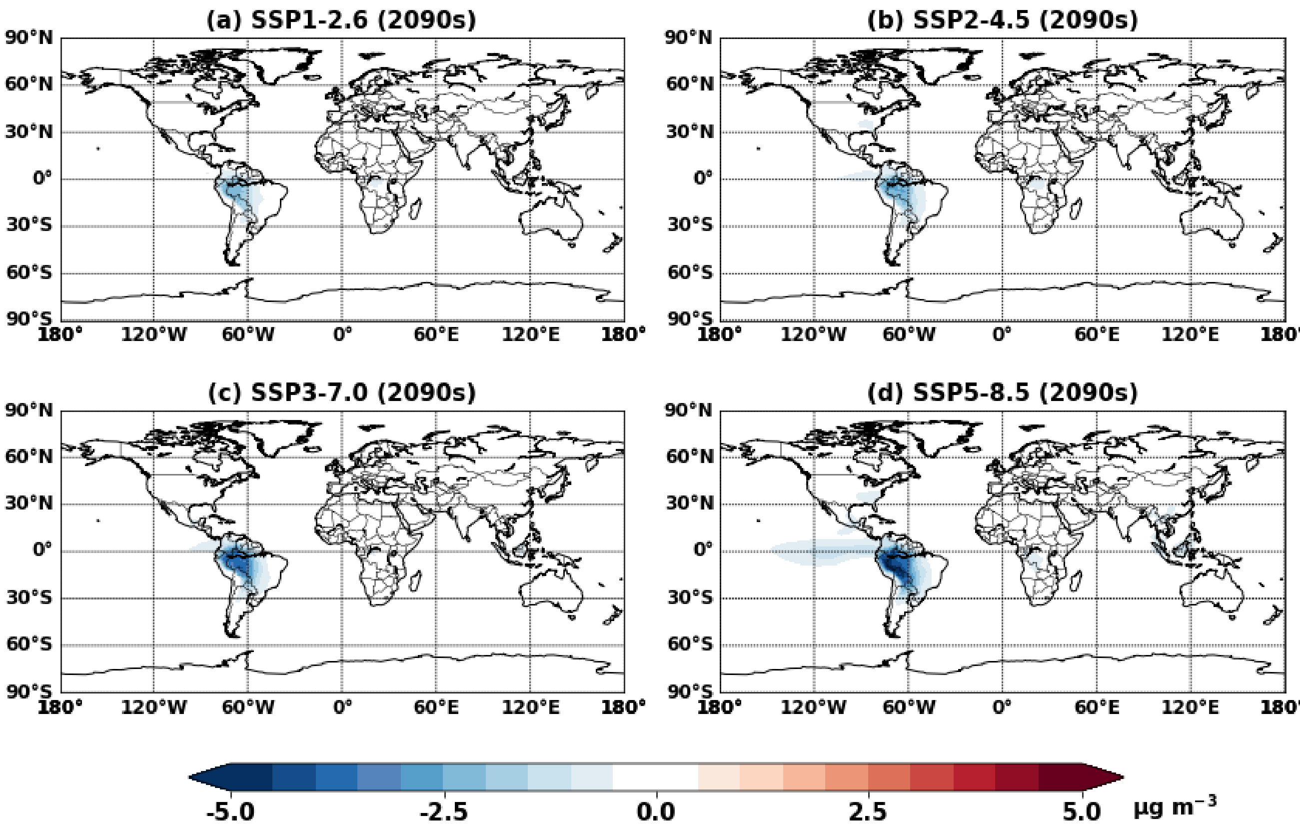

Figure S17. Simulated IEPOX-SOA concentration changes at the surface by including sea salt in aerosol thermodynamic calculation (EXP_SS_2090 - EXP_2090).

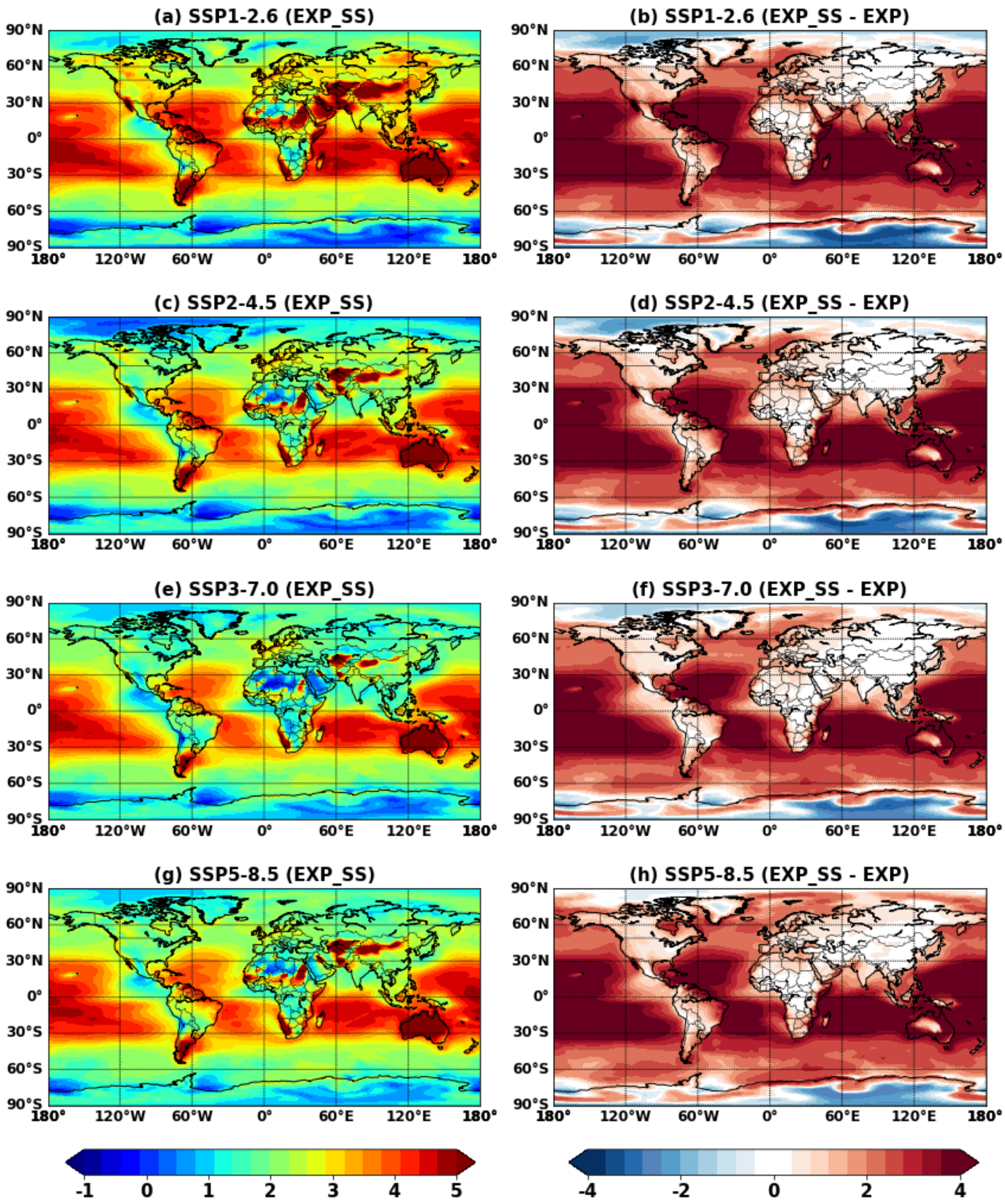

Figure S18. The multi-year mean global aerosol pH (accumulation mode) of EXP_SS_2090 simulations at the surface (left column) and pH differences between EXP_SS_2090 and EXP_2090 simulations.

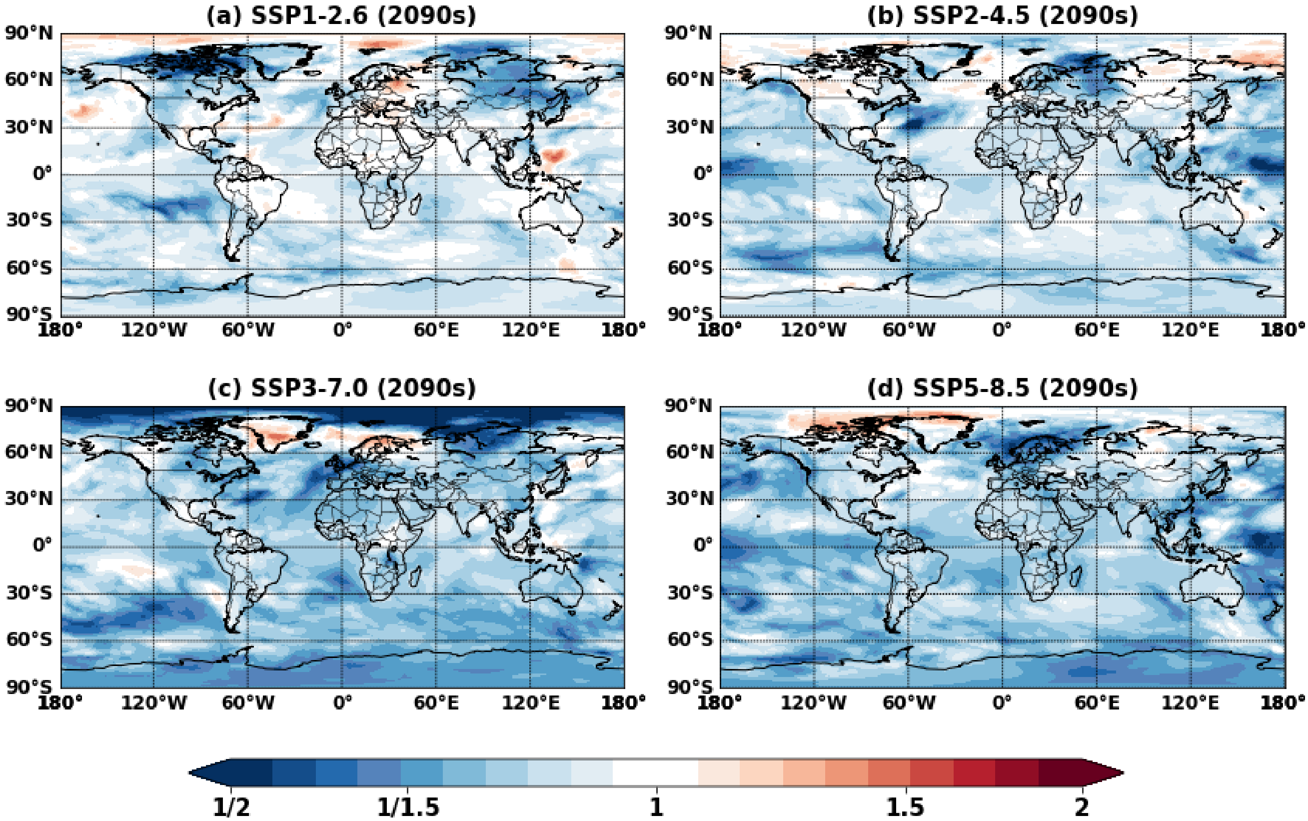

Figure S19. Global ratio maps of surface mean IEPOX-SOA concentrations between EXP_2090_CO2 (with CO_2 inhibition) and EXP_2090 (without CO_2 inhibition) for different SSP scenarios.

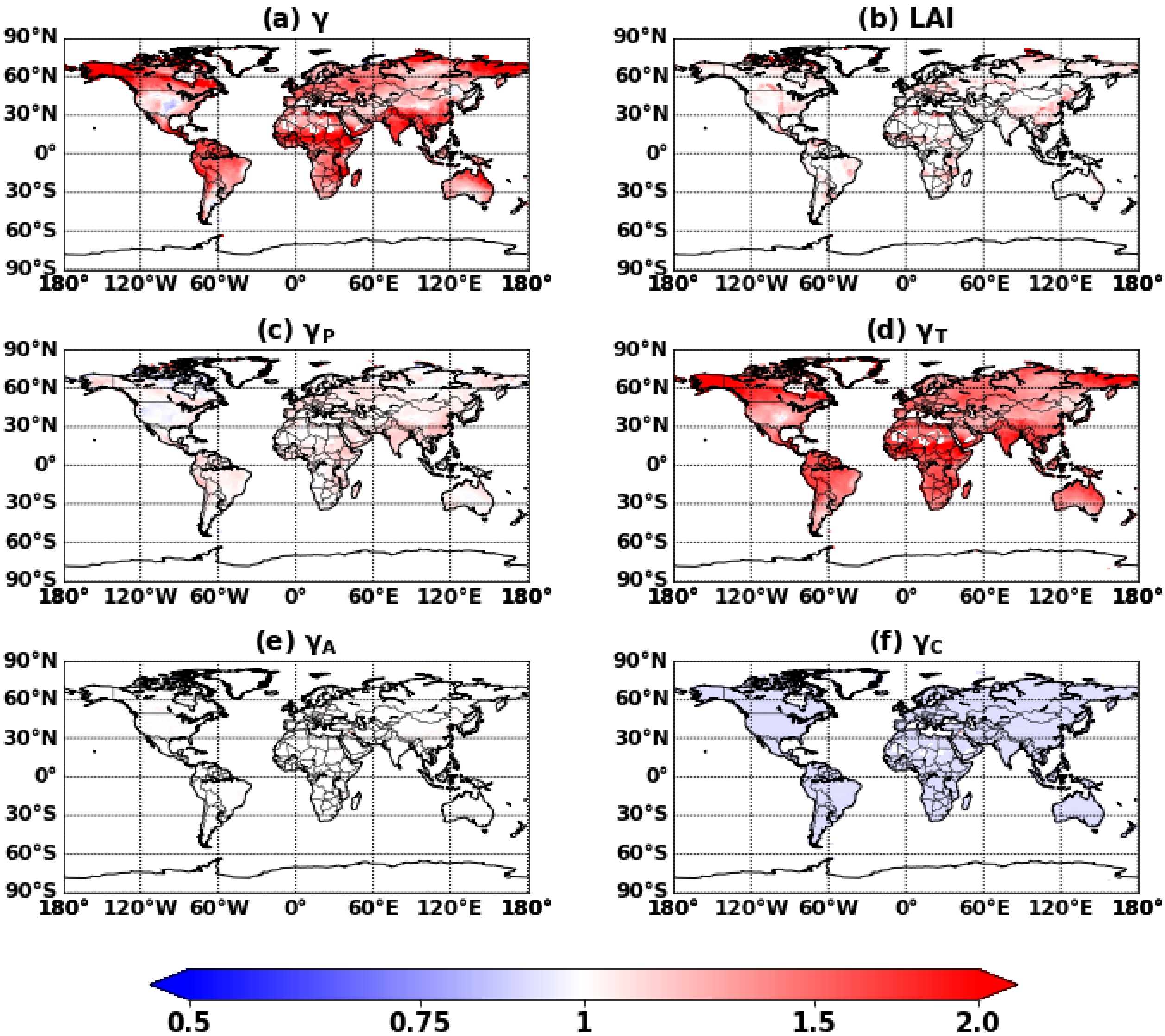

Figure S20. Global maps of activity factor changes (ratio of SSP1-2.6 to present) used in isoprene emission calculations by MEGANv2.1. (a) total activity factor (γ), (b) leaf area index (LAI), (c) emission response to light (γ_P), (d) temperature (γ_T), (e) leaf age (γ_A), and (f) CO_2 inhibition. See Eq. (2) in Guenther et al. (2012) for details. Soil moisture factor is not included, as CESM2.1.0 applies a unity value for soil moisture factor.

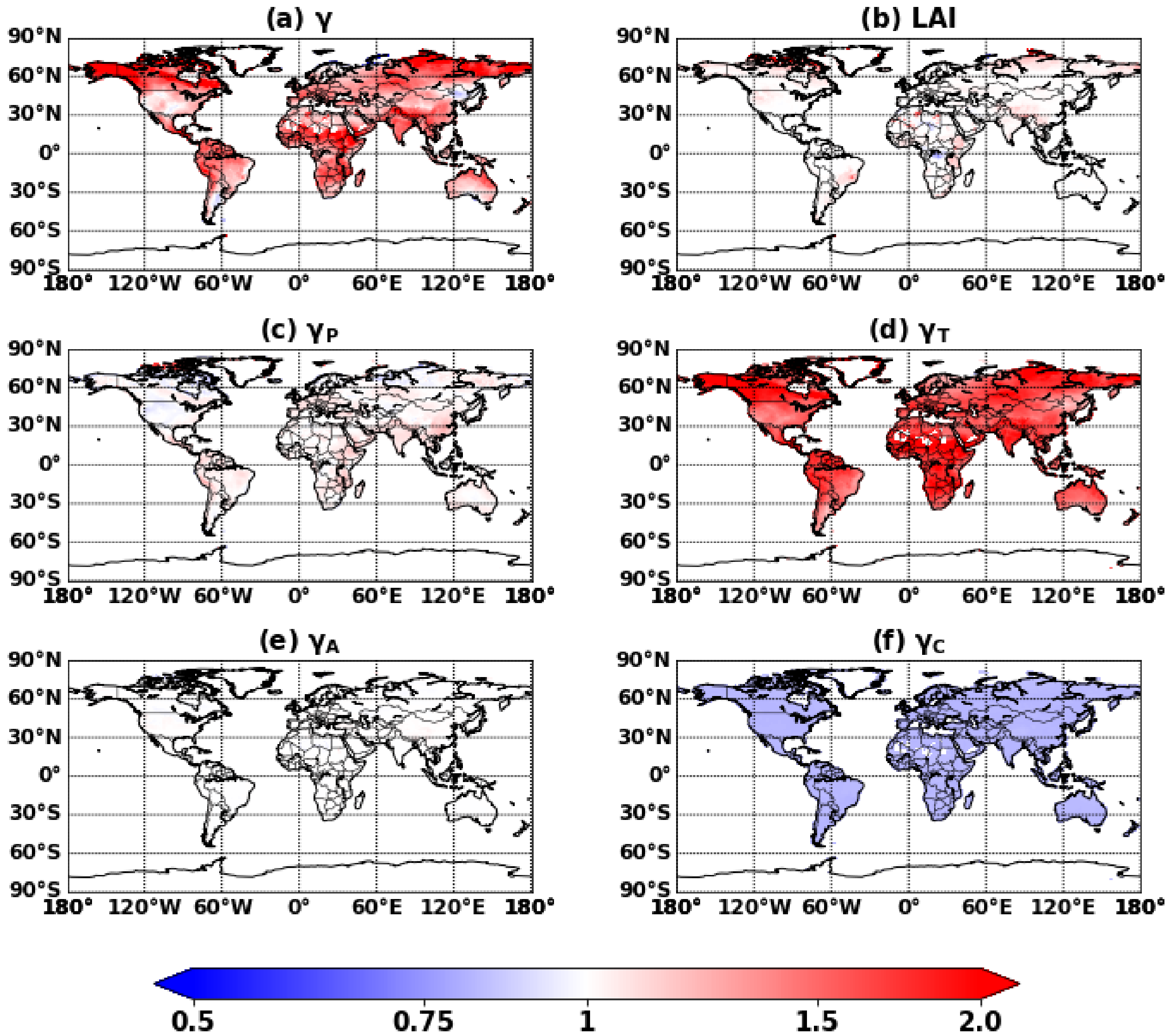

Figure S21. Same as Fig. S20 but for the SSP5-8.5 scenario.

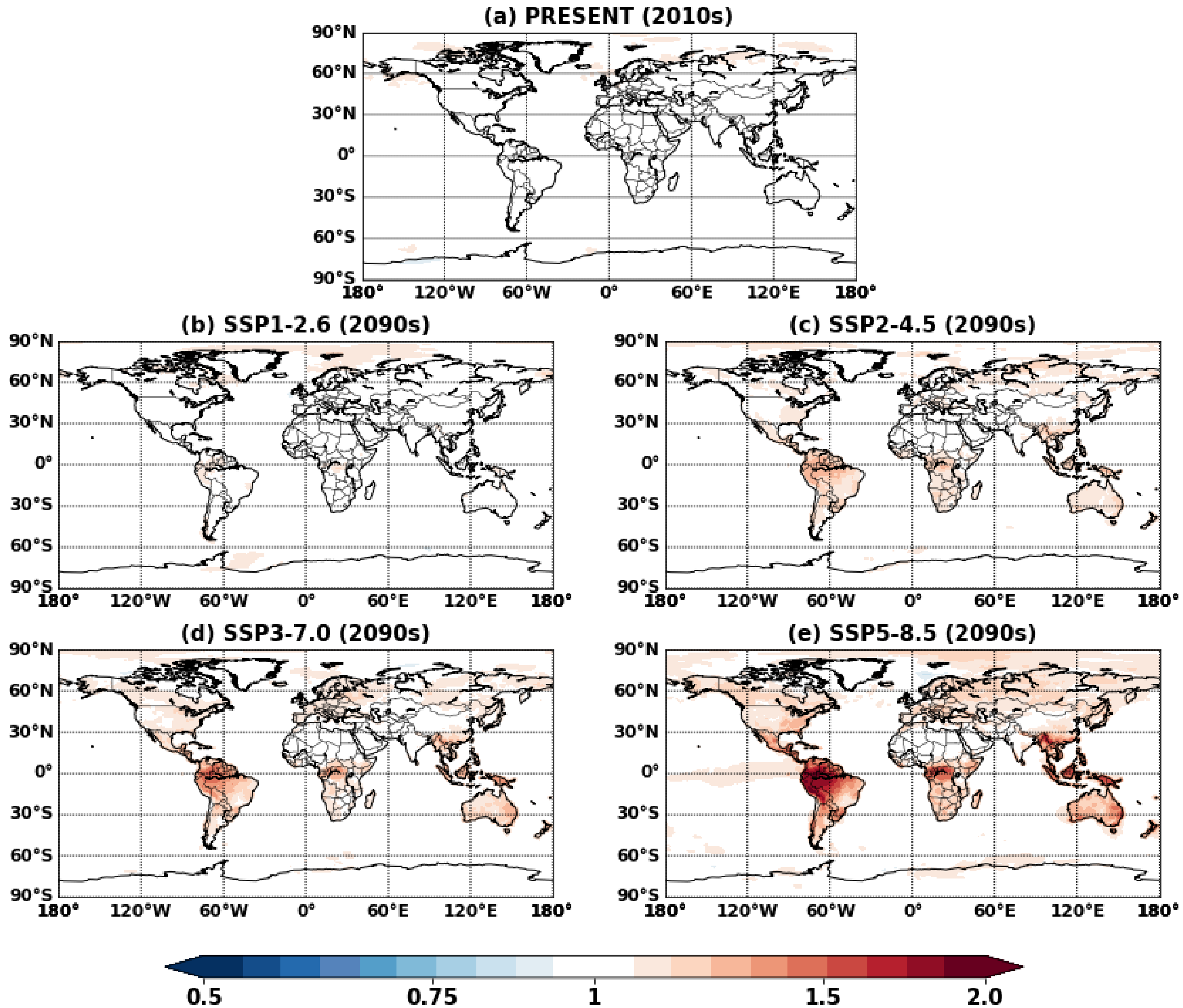

Figure S22. Global ratio maps of OH concentrations between simulations with (EXP) and without CO_2 (EXP_CO2) inhibition effects.

Table S1. A brief summary of SSP scenarios used in this study. Values are for the year 2100. For more information, readers are referred to previous studies (O'Neill et al., 2016; Riahi et al., 2017; Kc and Lutz, 2017; Gidden et al., 2019; Feng et al., 2020).

SSP1-2.6	Title[1)]	Sustainability - Taking the Green Road (Low challenges to mitigation and adaptation)
	Description[1)]	The world shifts gradually, but pervasively, toward a more sustainable path, emphasizing more inclusive development that respects perceived environmental boundaries. Management of the global commons slowly improves, educational and health investments accelerate the demographic transition, and the emphasis on economic growth shifts toward a broader emphasis on human well-being. Driven by an increasing commitment to achieving development goals, inequality is reduced both across and within countries. Consumption is oriented toward low material growth and lower resource and energy intensity.
	Forcing category[2)]	Low
	Target forcing level[2)] ($W\ m^{-2}$)	2.6
	Population[3)] (millions)	6,881
	Land use change regulation[1)]	strong
	Sulfur emissions[4)] ($Mt\ SO_2\ yr^{-1}$)	8.1
	NO_x emissions[4)] ($Mt\ NO_2\ yr^{-1}$)	41.2
	VOC emissions[4)] ($Mt\ VOC\ yr^{-1}$)	62.3
	OC emissions[4)] ($Mt\ OC\ yr^{-1}$)	13.1
	CO_2 emissions[4)] ($Mt\ CO_2\ yr^{-1}$)	-8,618
SSP2-4.5	Title[1)]	Middle of the Road (Medium challenges to mitigation and adaptation)

	Description[1)]	The world follows a path in which social, economic, and technological trends do not shift markedly from historical patterns. Development and income growth proceeds unevenly, with some countries making relatively good progress while others fall short of expectations. Global and national institutions work toward but make slow progress in achieving sustainable development goals. Environmental systems experience degradation, although there are some improvements and overall the intensity of resource and energy use declines. Global population growth is moderate and levels off in the second half of the century. Income inequality persists or improves only slowly and challenges to reducing vulnerability to societal and environmental changes remain.
	Forcing category[2)]	Medium
	Target forcing level[2)] ($W\ m^{-2}$)	4.5
	Population[3)] (millions)	9,000
	Land use change regulation[1)]	medium
	Sulfur emissions[4)] ($Mt\ SO_2\ yr^{-1}$)	30.8
	NO_x emissions[4)] ($Mt\ NO_2\ yr^{-1}$)	77.7
	VOC emissions[4)] ($Mt\ VOC\ yr^{-1}$)	120.7
	OC emissions[4)] ($Mt\ OC\ yr^{-1}$)	14.5
	CO_2 emissions[4)] ($Mt\ CO_2\ yr^{-1}$)	9,683
SSP3-7.0	Title[1)]	Regional Rivalry – A Rocky Road (High challenges to mitigation and adaptation)

	Description[1)]	A resurgent nationalism, concerns about competitiveness and security, and regional conflicts push countries to increasingly focus on domestic or, at most, regional issues. Policies shift over time to become increasingly oriented toward national and regional security issues. Countries focus on achieving energy and food security goals within their own regions at the expense of broader-based development. Investments in education and technological development decline. Economic development is slow, consumption is material-intensive, and inequalities persist or worsen over time. Population growth is low in industrialized and high in developing countries. A low international priority for addressing environmental concerns leads to strong environmental degradation in some regions.
	Forcing category[2)]	High
	Target forcing level[2)] ($W\ m^{-2}$)	7.0
	Population[3)] (millions)	12,627
	Land use change regulation[1)]	weak
	Sulfur emissions[4)] (Mt SO_2 yr^{-1})	78.1
	NO_x emissions[4)] (Mt NO_2 yr^{-1})	144.4
	VOC emissions[4)] (Mt VOC yr^{-1})	227.9
	OC emissions[4)] (Mt OC yr^{-1})	33.7
	CO_2 emissions[4)] (Mt CO_2 yr^{-1})	82,726
SSP5-8.5	Title[1)]	Fossil-fueled Development – Taking the Highway (High challenges to mitigation, low challenges to adaptation)

	Description[1)]	This world places increasing faith in competitive markets, innovation and participatory societies to produce rapid technological progress and development of human capital as the path to sustainable development. Global markets are increasingly integrated. There are also strong investments in health, education, and institutions to enhance human and social capital. At the same time, the push for economic and social development is coupled with the exploitation of abundant fossil fuel resources and the adoption of resource and energy intensive lifestyles around the world. All these factors lead to rapid growth of the global economy, while global population peaks and declines in the 21st century. Local environmental problems like air pollution are successfully managed. There is faith in the ability to effectively manage social and ecological systems, including by geo-engineering if necessary.
	Forcing category[2)]	High
	Target forcing level[2)] ($W\ m^{-2}$)	8.5
	Population[3)] (millions)	7,363
	Land use change regulation[1)]	medium
	Sulfur emissions[4)] ($Mt\ SO_2\ yr^{-1}$)	29.5
	NO_x emissions[4)] ($Mt\ NO_2\ yr^{-1}$)	98.7
	VOC emissions[4)] ($Mt\ VOC\ yr^{-1}$)	163.3
	OC emissions[4)] ($Mt\ OC\ yr^{-1}$)	17.6
	CO_2 emissions[4)] ($Mt\ CO_2\ yr^{-1}$)	126,287

1) Riahi et al. (2017); 2) O'Neill et al. (2016); 3) KC and Lutz (2017); 4) Gidden et al. (2019)

Table S2. Datasets used in Sect. 3.3 and Fig. 4[a]. Ranges or average plus standard deviation of $f_{C_5H_6O}$ (high resolution) and f_{82} (unit mass resolution) in different studies are also included.

Name of datasets	Time Period	Site locations and descriptions	Campaign name	Ranges or average±std.dev. f_{C5H6O} (‰)	Ranges or average±std.dev. f_{82} (‰)	OA Conc. (ug/m3)	IEPOX-SOA Conc. (ug/m3)	IEPOX-SOA/OA (%)	Latitude	longitude	Ref.	X axis label in Fig. 4
Studies strongly-influenced by isoprene emissions under lower NO												
SE US forest - CTR site, 2013 SOAS	Jun-Jul, 2013	Centreville, AL	SOAS	6.2±2.4	7.6±2.2	3.8	0.64	17	32.95	-87.13	-1	Centreville 2013 Summer
SE US forest - Look Rock site, 2013 SOAS	Jun-Jul, 2013	Look Rook	SOAS	N/A	N/A	4.87	1.6	33	35.61	-83.55	-2	N/A[c]
SE US forest - Look Rock site, 2013 Spring	Mar-May, 2013	Look Rock	N/A	N/A	N/A	3.23	1.32	41	35.61	-83.55	-3	Look Rock, 2013 Spring
SE US forest - Look Rock site, 2013 Summer	Jun-Sep, 2013	Look Rock	N/A	N/A	N/A	5.32	2.13	40	35.61	-83.55	-3	Look Rock, 2013 Summer
SE US forest - Look Rock site, 2013 Fall	Oct-Dec, 2013	Looak Rock	N/A	N/A	N/A	2.83	0.76	27	35.61	-83.55	-3	Look Rock, 2013 Fall
Atlanta JST site, 2012 Spring	Mar-Jun, 2012	Urban JST site, Atlanta, Georgia, US	N/A	N/A	N/A	4.7	1.74	37	33.78	-84.42	-3	Atlanta (JST), 2012 Spring
Atlanta JST site, 2013 Summer	Jul-Sep, 2013	Urban JST site, Atlanta, Georgia, US	N/A	N/A	N/A	6.15	2.34	38	33.78	-84.42	-3	Atlanta (JST), 2013 Summer
Atlanta JST site, 2014 Spring	May-Jun, 2014	Urban JST site, Atlanta, Georgia, US	N/A	N/A	N/A	9.61	2.4	25	33.78	-84.42	-4	Atlanta (JST), 2014 Spring
Atlanta JST site, 2014 Summer	Jul-Sep, 2014	Urban JST site, Atlanta, Georgia, US	N/A	N/A	N/A	11.36	3.29	29	33.78	-84.42	-4	Atlanta (JST), 2014 Summer
Pristine Amazon forest 2008, Brazil	Feb-Mar, 2008	Pristine rain forest site, TT34	AMAZE-08	5.0±2.3	7.9±1.7	0.76	0.26	34	-2.59	-60.2	-5	Amazon, 2008 Summer

Amazon forest downwind Manaus, Brazil	Feb-Mar, 2014	T3 site, near Manacapuru	GoAmazon2014/5	6.9±1.6	7.1±1.0	1.3	0.286	22	-3.21	-60.59	-6	Amazon, 2014 Summer
Pristine Amazon forest 2014, Brazil	Aug-Dec, 2014	T0 site, ~150 km northeast of Manaus	GoAmazon2014/5	N/A	5.6±1.7	N/A	N/A	N/A	-3.21	-60.59	-7	N/A
SEAC4RS	Aug-Sep, 2013	Aircraft measurement	SEAC4RS	4.3±1.6	N/A	N/A	N/A	32	Flight track	Flight track	-8	N/A
Borneo forest, Malaysia	Jun-Jul, 2008	Rain forest GAW station, Sabah, Malaysia	OP3	10±0.3	12.4±0.4	0.75	0.18	24	4.981	117.844	-9	Borneo, 2008 Summer
Atlanta JST site, 2011 Summer	Aug-Sep, 2011	Urban JST site, Atlanta, Georgia, US	N/A	N/A	3.7±1.9	11.6	3.8	33	33.78	-84.42	-10	Atlanta (JST), 2011 Summer
Atlanta JST site, 2012 May	May, 2012	Urban JST site, Atlanta, Georgia, US	N/A	3.3±0.9	N/A	9.1	1.91	21	33.78	-84.42	-11	N/A[d]
Atlanta GT site, 2012 Summer	Aug, 2012	Urban Georgia Tech site, Georgia, US	N/A	5.4±1.9	N/A	9.6	3	31	33.78	-84.396	-11	Atlanta (GT), 2012 Summer
Yorkville, 2012 Summer	July, 2012	Rural sites, 80km northwest of JST site, Georgia, US	N/A	7.7±2.2	N/A	11.2	4	36	33.9285	-85.045	-11	Yorkville, 2012 Summer
Harrow, Canada	Jun-Jul, 2007	Harrow site, rural sites surrounded by farmland, Canada	BAQSMET	N/A	N/A	N/A	N/A	17	42.03	-82.9	-12	N/A
Bear Creek, Canada	Jun-Jul, 2007	Bear Creek site, wetlands area surrounded by farmland, Canada	BAQSMET	N/A	N/A	N/A	N/A	6	42.51	-82.34	-12	N/A
Studies strongly-influenced by monoterpene emissions												
Rocky mountain pine forest, CO, USA	Jul-Aug, 2011	Manitou Experimental Forest Observatory, CO,	BEACHON-RoMBAS	3.7±0.5	5.1±0.5	N/A	N/A	N/A	39.1	-105.1	-13	N/A
European Boreal forest, Finland	2008-2009	Hyytiala site in Pine forest, Finland	EUCAARI campaign	2.5±0.1 [b]	4.8±0.1 [b]	N/A	N/A	N/A	61.85	24.28	-9	N/A

Studies mixed-influenced by isoprene and monoterpene emissions												
North American temperate, US	Aug-Sep, 2007	Blodgett Forest Ameriflux Site, CA, US	BEARPEX	4.0±<0.1 [b]	4.0±<0.1 [b]	N/A	N/A	N/A	N/A	N/A	-9	N/A
Studies strongly-influenced by urban emissions												
Los Angeles area , CA, USA	May-Jun, 2010	Pasadena, US	CalNex	1.6±0.2	3.6±0.5	7	<DL	< PMF limit	34.14	-118.12	-14	Pasadena 2010 Spring
Beijing, China	Nov-Dec, 2010	Peking University, in NW of Beijing city, China	N/A	1.5±0.3	4.6±0.7	34.5	<DL	< PMF limit	39.99	116.31	-15	Beijing 2010 Winter
Changdao island, Downwind of China	Mar-Apr, 2011	Changdao island, China	CAPTAIN	1.6±0.2	3.8±0.5	13.4	<DL	< PMF limit	37.99	120.7	-16	Changdao 2011 Spring
Barcelona area, Spain	Feb-Mar, 2009	Montseny, Spain	DAURE	1.6±0.2	4.8±0.9	N/A	<DL	< PMF limit	41.38	2.1	-17	Montseny 2009 Spring

a- HR-ToF-AMS was used for all the campaigns except the Atlanta, US, Look Rock, US, and Pristine Amazon forest 2014, Brazil using ACSM.

b- Standard error

c- included in Look Rock 2013 Summer

d- included in Atlanta (JST) 2012 Spring

(1)(Hu et al., 2015b); (2)(Budisulistiorini et al., 2015); (3)(Budisulistiorini et al., 2016); (4)(Rattanavaraha et al., 2017); (5)(Chen et al., 2014); (6)(de Sá et al., 2017); (7)(Carbone et al., 2015); (8)(Liao et al., 2014) ; (9)(Robinson et al., 2011); (10)(Budisulistiorini et al., 2013); (11)(Xu et al., 2014; Xu et al., 2015); (12)(Slowik et al., 2011); (13)(Ortega et al., 2014); (14)(Hayes et al., 2013); (15)(Hu et al., 2015a); (16)(Hu et al., 2013); (17)(Minguillón et al., 2011)

References

Bauwens, M., Stavrakou, T., Müller, J.-F., Smedt, I. D., Van Roozendael, M., Werf, G. R. van der, Wiedinmyer, C., Kaiser, J. W., Sindelarova, K. and Guenther, A.: Nine years of global hydrocarbon emissions based on source inversion of OMI formaldehyde observations, Atmos. Chem. Phys., 16(15), 10133–10158, 2016.

Budisulistiorini, S. H., Canagaratna, M. R., Croteau, P. L., Marth, W. J., Baumann, K., Edgerton, E. S., Shaw, S. L., Knipping, E. M., Worsnop, D. R., Jayne, J. T., Gold, A. and Surratt, J. D.: Real-time continuous characterization of secondary organic aerosol derived from isoprene epoxydiols in downtown Atlanta, Georgia, using the Aerodyne Aerosol Chemical Speciation Monitor, Environ. Sci. Technol., 47(11), 5686–5694, 2013.

Budisulistiorini, S. H., Li, X., Bairai, S. T., Renfro, J., Liu, Y., Liu, Y. J., McKinney, K. A., Martin, S. T., McNeill, V. F., Pye, H. O. T., Nenes, A., Neff, M. E., Stone, E. A., Mueller, S., Knote, C., Shaw, S. L., Zhang, Z., Gold, A. and Surratt, J. D.: Examining the effects of anthropogenic emissions on isoprene-derived secondary organic aerosol formation during the 2013 Southern Oxidant and Aerosol Study (SOAS) at the Look Rock, Tennessee ground site, Atmos. Chem. Phys., 15(15), 8871–8888, 2015.

Budisulistiorini, S. H., Baumann, K., Edgerton, E. S., Bairai, S. T., Mueller, S., Shaw, S. L., Knipping, E. M., Gold, A. and Surratt, J. D.: Seasonal characterization of submicron aerosol chemical composition and organic aerosol sources in the southeastern United States: Atlanta, Georgia,and Look Rock, Tennessee, Atmos. Chem. Phys., 16(8), 5171–5189, 2016.

Carbone, S., De Brito, J. F., Andreae, M., Pöhlker, C., Chi, X., Saturno, J., Barbosa, H., and Artaxo, P.: Preliminary characterization of submicron secondary aerosol in the amazon forest –ATTO station, in preparation, 2015.

Chen, Q., Farmer, D. K., Rizzo, L. V., Pauliquevis, T., Kuwata, M., Karl, T. G., Guenther, A., Allan, J. D., Coe, H., Andreae, M. O., Pöschl, U., Jimenez, J. L., Artaxo, P. and Martin, S. T.: Submicron particle mass concentrations and sources in the Amazonian wet season (AMAZE-08), Atmos. Chem. Phys., 15(7), 3687–3701, 2015.

Gidden, M. J., Riahi, K., Smith, S. J., Fujimori, S., Luderer, G., Kriegler, E., van Vuuren, D. P., van den Berg, M., Feng, L., Klein, D., Calvin, K., Doelman, J. C., Frank, S., Fricko, O., Harmsen, M., Hasegawa, T., Havlik, P., Hilaire, J., Hoesly, R., Horing, J., Popp, A., Stehfest, E. and Takahashi, K.: Global emissions pathways under different socioeconomic scenarios for use in CMIP6: a dataset of harmonized emissions trajectories through the end of the century, Geoscientific Model Development, 12(4), 1443–1475, 2019.

Guenther, A. B., Jiang, X., Heald, C. L., Sakulyanontvittaya, T., Duhl, T., Emmons, L. K. and Wang, X.: The Model of Emissions of Gases and Aerosols from Nature version 2.1 (MEGAN2.1): an extended and updated framework for modeling biogenic emissions, Geoscientific Model Development, 5(6), 1471–1492, 2012.

Hayes, P. L., Ortega, A. M., Cubison, M. J., Froyd, K. D., Zhao, Y., Cliff, S. S., Hu, W. W., Toohey, D. W., Flynn, J. H., Lefer, B. L., Grossberg, N., Alvarez, S., Rappenglück, B., Taylor, J. W., Allan, J. D., Holloway, J. S., Gilman, J. B., Kuster, W. C., de Gouw, J. A., Massoli, P., Zhang, X., Liu, J., Weber, R. J., Corrigan, A. L., Russell, L. M., Isaacman, G., Worton, D. R., Kreisberg, N. M., Goldstein, A. H., Thalman, R., Waxman, E. M., Volkamer, R., Lin, Y. H., Surratt, J. D., Kleindienst, T. E., Offenberg, J. H., Dusanter, S., Griffith, S., Stevens, P. S., Brioude, J., Angevine, W. M. and Jimenez, J. L.: Organic aerosol composition and sources in Pasadena, California, during the 2010 CalNex campaign: AEROSOL COMPOSITION IN PASADENA, J. Geophys. Res. D: Atmos., 118(16), 9233–9257, 2013.

Hu, W., Hu, M., Hu, W., Jimenez, J. L., Yuan, B., Chen, W., Wang, M., Wu, Y., Chen, C., Wang, Z., Peng, J., Zeng, L. and Shao, M.: Chemical composition, sources, and aging process of submicron aerosols in Beijing: Contrast between summer and winter: PM POLLUTION IN BEIJING, J. Geophys. Res. D: Atmos., 121(4), 1955–1977, 2016.

Hu, W. W., Hu, M., Yuan, B., Jimenez, J. L., Tang, Q., Peng, J. F., Hu, W., Shao, M., Wang, M., Zeng, L. M., Wu, Y. S., Gong, Z. H., Huang, X. F. and He, L. Y.: Insights on organic aerosol aging and the influence of coal combustion at a regional receptor site of central eastern China, Atmos. Chem. Phys., 13(19), 10095–10112, 2013.

Hu, W. W., Campuzano-Jost, P., Palm, B. B., Day, D. A., Ortega, A. M., Hayes, P. L., Krechmer, J. E., Chen, Q., Kuwata, M., Liu, Y. J., Sá, S. S. de, McKinney, K., Martin, S. T., Hu, M., Budisulistiorini, S. H., Riva, M., Surratt, J. D., Clair, J. M. S., Isaacman-Van Wertz, G., Yee, L. D., Goldstein, A. H., Carbone, S., Brito, J., Artaxo, P., Gouw, J. A. de, Koss, A., Wisthaler, A., Mikoviny, T., Karl, T., Kaser, L., Jud, W., Hansel, A., Docherty, K. S., Alexander, M. L., Robinson, N. H., Coe, H., Allan, J. D., Canagaratna, M. R., Paulot, F. and Jimenez, J. L.: Characterization of a real-time tracer for isoprene epoxydiols-derived secondary organic aerosol (IEPOX-SOA) from aerosol mass spectrometer measurements, Atmos. Chem. Phys., 15(20), 11807–11833, 2015.

Kc, S. and Lutz, W.: The human core of the shared socioeconomic pathways: Population scenarios by age, sex and level of education for all countries to 2100, Glob. Environ. Change, 42, 181–192, 2017.

Liao, J., Froyd, K. D., Murphy, D. M., Keutsch, F. N., Yu, G., Wennberg, P. O., St Clair, J. M., Crounse, J. D., Wisthaler, A., Mikoviny, T., Jimenez, J. L., Campuzano-Jost, P., Day, D. A., Hu, W., Ryerson, T. B., Pollack, I. B., Peischl, J., Anderson, B. E., Ziemba, L. D., Blake, D. R., Meinardi, S. and Diskin, G.: Airborne measurements of organosulfates over the continental U.S, J. Geophys. Res. D: Atmos., 120(7), 2990–3005, 2015.

Minguillón, M. C., Perron, N., Querol, X., Szidat, S., Fahrni, S. M., Alastuey, A., Jimenez, J. L., Mohr, C., Ortega, A. M., Day, D. A., Lanz, V. A., Wacker, L., Reche, C., Cusack, M., Amato, F., Kiss, G., Hoffer, A., Decesari, S., Moretti, F., Hillamo, R., Teinilä, K., Seco, R., Peñuelas, J., Metzger, A., Schallhart, S., Müller, M., Hansel, A., Burkhart, J. F., Baltensperger, U. and Prévôt, A. S. H.: Fossil versus contemporary sources of fine elemental and organic carbonaceous particulate matter during the DAURE campaign in Northeast Spain, Atmos.

Chem. Phys., 11(23), 12067–12084, 2011.

O'Neill, B. C., Tebaldi, C., van Vuuren, D. P., Eyring, V., Friedlingstein, P., Hurtt, G., Knutti, R., Kriegler, E., Lamarque, J.-F., Lowe, J., Meehl, G. A., Moss, R., Riahi, K. and Sanderson, B. M.: The Scenario Model Intercomparison Project (ScenarioMIP) for CMIP6, Geoscientific Model Development, 9(9), 3461–3482, 2016.

Ortega, J., Turnipseed, A., Guenther, A. B., Karl, T. G., Day, D. A., Gochis, D., Huffman, J. A., Prenni, A. J., Levin, E. J. T., Kreidenweis, S. M., DeMott, P. J., Tobo, Y., Patton, E. G., Hodzic, A., Cui, Y. Y., Harley, P. C., Hornbrook, R. S., Apel, E. C., Monson, R. K., Eller, A. S. D., Greenberg, J. P., Barth, M. C., Campuzano-Jost, P., Palm, B. B., Jimenez, J. L., Aiken, A. C., Dubey, M. K., Geron, C., Offenberg, J., Ryan, M. G., Fornwalt, P. J., Pryor, S. C., Keutsch, F. N., DiGangi, J. P., Chan, A. W. H., Goldstein, A. H., Wolfe, G. M., Kim, S., Kaser, L., Schnitzhofer, R., Hansel, A., Cantrell, C. A., Mauldin, R. L. and Smith, J. N.: Overview of the Manitou Experimental Forest Observatory: site description and selected science results from 2008 to 2013, Atmos. Chem. Phys., 14(12), 6345–6367, 2014.

Rattanavaraha, W., Canagaratna, M. R., Budisulistiorini, S. H., Croteau, P. L., Baumann, K., Canonaco, F., Prevot, A. S. H., Edgerton, E. S., Zhang, Z., Jayne, J. T., Worsnop, D. R., Gold, A., Shaw, S. L. and Surratt, J. D.: Source apportionment of submicron organic aerosol collected from Atlanta, Georgia, during 2014–2015 using the aerosol chemical speciation monitor (ACSM), Atmos. Environ., 167, 389–402, 2017.

Riahi, K., van Vuuren, D. P., Kriegler, E., Edmonds, J., O'Neill, B. C., Fujimori, S., Bauer, N., Calvin, K., Dellink, R., Fricko, O., Lutz, W., Popp, A., Cuaresma, J. C., Kc, S., Leimbach, M., Jiang, L., Kram, T., Rao, S., Emmerling, J., Ebi, K., Hasegawa, T., Havlik, P., Humpenöder, F., Da Silva, L. A., Smith, S., Stehfest, E., Bosetti, V., Eom, J., Gernaat, D., Masui, T., Rogelj, J., Strefler, J., Drouet, L., Krey, V., Luderer, G., Harmsen, M., Takahashi, K., Baumstark, L., Doelman, J. C., Kainuma, M., Klimont, Z., Marangoni, G., Lotze-Campen, H., Obersteiner, M., Tabeau, A. and Tavoni, M.: The Shared Socioeconomic Pathways and their energy, land use, and greenhouse gas emissions implications: An overview, Glob. Environ. Change, 42, 153–168, 2017.

Robinson, N. H., Hamilton, J. F., Allan, J. D., Langford, B., Oram, D. E., Chen, Q., Docherty, K., Farmer, D. K., Jimenez, J. L., Ward, M. W., Hewitt, C. N., Barley, M. H., Jenkin, M. E., Rickard, A. R., Martin, S. T., McFiggans, G. and Coe, H.: Evidence for a significant proportion of Secondary Organic Aerosol from isoprene above a maritime tropical forest, Atmos. Chem. Phys., 11(3), 1039–1050, 2011.

Sá, S. S. de, Palm, B. B., Campuzano-Jost, P., Day, D. A., Newburn, M. K., Hu, W., Isaacman-VanWertz, G., Yee, L. D., Thalman, R., Brito, J., Carbone, S., Artaxo, P., Goldstein, A. H., Manzi, A. O., Souza, R. A. F., Mei, F., Shilling, J. E., Springston, S. R., Wang, J., Surratt, J. D., Alexander, M. L., Jimenez, J. L. and Martin, S. T.: Influence of urban pollution on the production of organic particulate matter from isoprene epoxydiols in central Amazonia, Atmos. Chem. Phys., 17(11), 6611–6629, 2017.

Slowik, J. G., Brook, J., Chang, R. Y.-W., Evans, G. J., Hayden, K., Jeong, C.-H., Li, S.-M., Liggio, J., Liu, P. S.

K., McGuire, M., Mihele, C., Sjostedt, S., Vlasenko, A. and Abbatt, J. P. D.: Photochemical processing of organic aerosol at nearby continental sites: contrast between urban plumes and regional aerosol, Atmos. Chem. Phys., 11(6), 2991–3006, 2011.

Xu, L., Suresh, S., Guo, H., Weber, R. J. and Ng, N. L.: Aerosol characterization over the southeastern United States using high-resolution aerosol mass spectrometry: spatial and seasonal variation of aerosol composition and sources with a focus on organic nitrates, Atmos. Chem. Phys., 15(13), 7307–7336, 2015a.

Xu, L., Guo, H., Boyd, C. M., Klein, M., Bougiatioti, A., Cerully, K. M., Hite, J. R., Isaacman-VanWertz, G., Kreisberg, N. M., Knote, C., Olson, K., Koss, A., Goldstein, A. H., Hering, S. V., de Gouw, J., Baumann, K., Lee, S.-H., Nenes, A., Weber, R. J. and Ng, N. L.: Effects of anthropogenic emissions on aerosol formation from isoprene and monoterpenes in the southeastern United States, Proc. Natl. Acad. Sci. U. S. A., 112(1), 37–42, 2015b.